



First detection of ammonia (NH₃) in the Asian summer monsoon upper troposphere

Michael Höpfner¹, Rainer Volkamer^{2,3}, Udo Grabowski¹, Michel Grutter⁴, Johannes Orphal¹, Gabriele Stiller¹, Thomas von Clarmann¹, and Gerald Wetzell¹

¹Institute of Meteorology and Climate Research, Karlsruhe Institute of Technology, Karlsruhe, Germany

²Department of Chemistry & Biochemistry, University of Colorado, Boulder, CO, USA

³Cooperative Institute for Research in Environmental Sciences, University of Colorado at Boulder, CO, USA

⁴Centro de Ciencias de la Atmósfera, Universidad Nacional Autónoma de México, Mexico City, Mexico

Correspondence to: Michael Höpfner (michael.hoepfner@kit.edu)

Received: 10 May 2016 – Published in Atmos. Chem. Phys. Discuss.: 3 June 2016

Revised: 19 October 2016 – Accepted: 25 October 2016 – Published: 18 November 2016

Abstract. Ammonia (NH₃) has been detected in the upper troposphere by the analysis of averaged MIPAS (Michelson Interferometer for Passive Atmospheric Sounding) infrared limb-emission spectra. We have found enhanced amounts of NH₃ within the region of the Asian summer monsoon at 12–15 km altitude. Three-monthly, 10° longitude × 10° latitude average profiles reaching maximum mixing ratios of around 30 pptv in this altitude range have been retrieved, with a vertical resolution of 3–8 km and estimated errors of about 5 pptv. These observations show that loss processes during transport from the boundary layer to the upper troposphere within the Asian monsoon do not deplete the air entirely of NH₃. Thus, ammonia might contribute to the so-called Asian tropopause aerosol layer by the formation of ammonium aerosol particles. On a global scale, outside the monsoon area and during different seasons, we could not detect enhanced values of NH₃ above the actual detection limit of about 3–5 pptv. This upper bound helps to constrain global model simulations.

in southeast China and northern India (Paulot et al., 2014; Van Damme et al., 2015).

Neutralization of acids by the alkaline gas NH₃ leads to the formation of ammonium salts in the atmosphere. For example, the reaction of NH₃ with sulfuric acid (H₂SO₄) or nitric acid (HNO₃) forms aerosol particles composed of ammonium sulfate ((NH₄)₂SO₄) or ammonium nitrate (NH₄NO₃) (e.g., Behera et al., 2013, and references therein). These inorganic aerosols are important not only with regard to air quality considerations (Hamaoui-Laguel et al., 2014) but they also affect climate through various direct and indirect radiative impacts (Adams et al., 2001; Martin et al., 2004; Liao and Seinfeld, 2005; Forster et al., 2007; Xu and Penner, 2012; Boucher et al., 2013). Further, cirrus clouds might also be affected by the presence of NH₃ and ammonium (Tabazadeh and Toon, 1998; Wang et al., 2008). For example, ammonium sulfate aerosols that are partially coated and have exposed surface sites are active with respect to ice nucleation (Prenni et al., 2001; Wise et al., 2004). Such a heterogeneous nucleation pathway might influence the size and number of cirrus particles and, consequently, their radiative impact (Abbatt et al., 2006). Moreover, through the stabilization of sulfuric acid clusters, ammonia itself may play an important role regarding the initial nucleation of sulfuric acid aerosols (Ortega et al., 2008; Kirkby et al., 2011; Schobesberger et al., 2013; Kürten et al., 2015).

Global emissions of NH₃ are expected to rise strongly due to the need to sustain a growing population and due to enhanced emissions under increasing tem-

1 Introduction

In the Earth's atmosphere the trace gas ammonia (NH₃) represents the major form of reduced nitrogen. With a share of around 70–80 %, the bulk of ammonia emissions is due to anthropogenic activity, namely the use of synthetic fertilizers and livestock manure management (Bouwman et al., 1997; Paulot et al., 2015). Major source regions of NH₃ are located

peratures (Erismann et al., 2008; Vuuren et al., 2011; Sutton et al., 2013). As a result, future prospects of a positive radiative forcing by a decrease in the shortwave albedo caused by reductions in industrial SO₂ emissions may partly be compensated for by increasing amounts of ammonium-containing aerosols (Bellouin et al., 2011; Xu and Penner, 2012; Shindell et al., 2013; Hauglustaine et al., 2014).

With regard to the predicted increase in NH₃ emissions and the possible compensating effect on aerosol radiative forcing, Paulot et al. (2016) emphasize the need to also better constrain the vertical distribution of ammonia. However, there is very little information from measurements on NH₃ at mid- and upper-tropospheric levels.

Before 2008, measurements of ammonia were almost exclusively based on in situ technologies (von Bobruzki et al., 2010). Compared to the wealth of observations on the ground, vertical profiles of NH₃ from in situ observations above the boundary layer are relatively sparse. Recently, aircraft-borne campaign measurements over the US obtained concentration profiles in the free troposphere reaching altitudes of about 6 km (Nowak et al., 2007, 2010, 2012; Leen et al., 2013; Schiferl et al., 2016). At these altitudes the maximum observed NH₃ mixing ratios reached about 800 pptv (Schiferl et al., 2016) with detection limits of 70 pptv (Nowak et al., 2010). In situ airborne observations over Germany by Ziereis and Arnold (1986) restricted concentrations to the sub-pptv range at altitudes between 8 and 10 km. To our knowledge, these are the only upper-tropospheric in situ measurements of NH₃ published so far.

A first step in the direction of observations with global coverage was achieved by Beer et al. (2008), who reported the detection of NH₃ in the lower troposphere from spaceborne nadir sounding measurements by the Tropospheric Emission Spectrometer (TES) on the Earth Observing System (EOS) Aura satellite. Subsequently, various papers have been published describing retrieval, validation and interpretation of NH₃ derived from the nadir sounders TES (Clarisse et al., 2010; Shephard et al., 2011), IASI (Infrared Atmospheric Sounding Interferometer) (Coheur et al., 2009; Clarisse et al., 2009, 2010; Van Damme et al., 2014), CrIS (Cross-track Infrared Sounder) (Shephard and Cady-Pereira, 2015), and AIRS (Atmospheric Infrared Sounder) (Warner et al., 2016). The vertical sensitivity of these satellite retrievals is mainly limited to the lower troposphere up to about 3–4 km, and no altitude resolution is achieved (e.g., Clarisse et al., 2010; Shephard and Cady-Pereira, 2015). Recently, retrievals of NH₃ vertical column amounts from ground-based Fourier transform infrared (FTIR) solar observations located at various sites have been presented by Dammers et al. (2015) and are being used for the quantitative validation of spaceborne nadir-viewing datasets (Dammers et al., 2016). As shown by Dammers et al. (2015) in the case of high amounts of NH₃ near the surface, the retrieval sensitivity peaks within the boundary layer where the altitude gradient can also be de-

rived. For low concentrations, the retrieval is only sensitive to the total vertical column amount.

To achieve vertically resolved profiles of trace gases in the upper troposphere and above, limb-sounding techniques have been applied frequently. Regarding ammonia, Oelhaf et al. (1983) reported upper limits of 100 pptv above 10 km by analysis of balloon-borne limb solar absorption spectra measured over the US. Space-borne solar occultation measurements obtained with the Atmospheric Chemistry Experiment Fourier Transform Spectrometer (ACE-FTS) instrument within a plume of biomass burning over Tanzania have been studied by Coheur et al. (2007). In that publication, the authors mention a “tentative identification” of NH₃ in the spectra, while the spectral signals of various other trace species, such as C₂H₄, C₃H₆O, H₂CO, and PAN, were detected unequivocally. Nonetheless, Coheur et al. (2007) derived a vertical profile of NH₃ between 6.5 and 17 km with typical values of less than 20 pptv and a maximum of about 50 pptv at 8 km. Burgess et al. (2006) report on first attempts to retrieve global distributions of ammonia using limb infrared emission spectra measured by the Michelson Interferometer for Passive Atmospheric Sounding (MIPAS) on Envisat. They obtained one climatological vertical profile with NH₃ volume mixing ratios below 5 pptv at altitudes above 9 km. However, no evidence of the presence of NH₃ in the limb spectra nor any indication of enhanced values within the area of the Asian summer monsoon is shown.

In summary, considering the reported observations, neither the in situ measurements by Ziereis and Arnold (1986) nor the limb-sounding remote-sensing data (Oelhaf et al., 1983; Coheur et al., 2007; Burgess et al., 2006) prove the presence of ammonia at altitudes above about 8 km. In the work presented below, we show, to our knowledge, the first evidence of NH₃ together with quantitative retrievals at upper-tropospheric levels by the use of MIPAS averaged limb spectra.

2 MIPAS/Envisat

On board the Envisat satellite, the MIPAS limb sounder recorded infrared spectra of the radiation emitted by atmospheric constituents from June 2002 until April 2012 (Fischer et al., 2008). Between June 2002 and March 2004 (period 1), the spectral resolution was 0.025 cm⁻¹, with one limb scan consisting of 17 spectra from about 6 to 60 km altitude with steps of 3 km up to about 42 km in the case of nominal-mode observations. From January 2005 until April 2012 (period 2), the spectral resolution was reduced to 0.0625 cm⁻¹. This was accompanied by a better vertical sampling (27 tangent levels up to about 70 km altitude with 1.5 km steps up to ≈ 23 km). Also in the horizontal direction along the satellite track, the sampling distance between consecutive limb scans improved from 550 km during period 1 to 420 km during period 2.

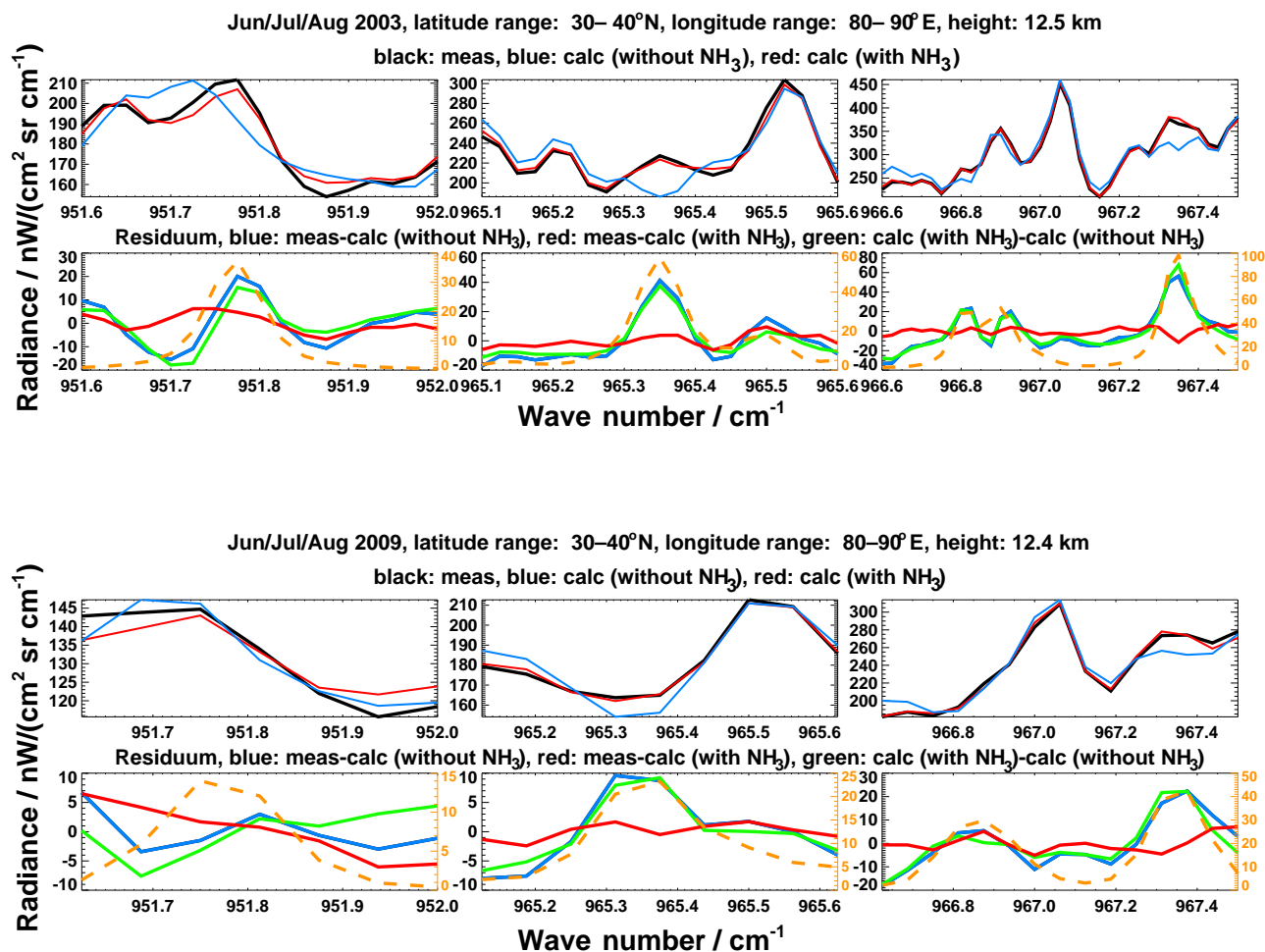


Figure 1. Spectral identification of NH₃ in MIPAS observations within the three spectral windows used for the retrieval (columns). The top two rows belong to the first observational period with higher spectral resolution. Rows 3 and 4 refer to the second period with lower spectral resolution. Rows 1 and 3 contain measured (black) and best-fit spectra (blue: without; red: with NH₃). Rows 2 and 4 show the spectral residuals without consideration of NH₃ (blue) and with NH₃ (red). Green curves in the second and fourth row represent the spectral features of NH₃ (calculation with NH₃ minus calculation without NH₃). To guide the eye, the orange dashed lines in rows 2 and 4 are simulated pure NH₃ spectra.

3 Retrieval and spectral detection

Here we report on the detection and retrieval of NH₃ from MIPAS observations in the upper troposphere on the basis of averaged limb spectra. This method has already been applied successfully for the detection of bromine nitrate (BrONO₂) (Höpfner et al., 2009) and for the compilation of a global climatology of stratospheric sulfur dioxide (SO₂) from MIPAS measurements (Höpfner et al., 2013). In those investigations the mean spectra consisted of monthly zonal averages within 10° latitude intervals, whereas for the present work we have chosen seasonal (3-monthly) averages within bins of 10° latitude by 10° longitude. Thus, we have refrained from zonal averaging in order to obtain resolution in the meridional direction, albeit slightly sacrificing temporal resolution. To reduce the spectral noise by at least a factor of 5, we have

chosen a lower limit of 25 single spectra (MIPAS level-1b version 5) for averaging. The resulting mean number of co-added spectra per time–latitude–longitude bin varies from 53 to 56 for the years 2003 and 2007 to 65–70 for 2008–2011 reaching maximum numbers of around 140 (see Supplement for the detailed geographical and temporal distribution). This leads to a typical reduction in the spectral noise by 0.1 ranging from 0.2 to 0.08 and signal-to-noise values resulting in retrieval errors near and below 1 pptv of NH₃ (see detailed error estimation below). In the troposphere the number of available spectra is limited as a result of cloud contamination along the limb line of sight. We have applied a cloud filter to deselect cloud-contaminated spectra before averaging. For the cloud detection scheme the established cloud index method (Spang et al., 2004) with a cloud index limit of 2.0 has been used.

Table 1. Assumptions on uncertainties used for the error assessment in Fig. 2.

Error source	Assumed uncertainty	Abbreviation
Spectral noise after apodization ¹	period 1: 2.2 (1.5–3.1) nW/ (cm ² sr cm ⁻¹) period 2: 1.3 (0.8–1.8) nW/ (cm ² sr cm ⁻¹)	noise
Instrument line shape ²	3 %	ils
Instrument gain calibration ³	1 %	gain
Tangent altitude ⁴	300 m	htang
Temperature ⁵	2 K below/ 5 K above 35 km	Tecm
Retrieval from averaged spectra ⁶		nlin
Air-broadened half width of NH ₃ lines ⁷	10 %	spe_hw_NH ₃
Intensity of NH ₃ lines ⁷	15 %	spe_int_NH ₃
Air-broadened half width of interfering gas lines ⁷	15 %	spe_hw_itf
Intensity of interfering gas lines ⁷	5 %	spe_int_itf

¹ ESA 11b dataset, depending on number of co-added spectra. ² F. Hase, personal communication, 2015; Höpfner et al. (2007).

³ Kleinert et al. (2007). ⁴ von Clarmann et al. (2003); Von Clarmann et al. (2009); Kiefer et al. (2007). ⁵ ECMWF uncertainty: Höpfner et al. (2013). ⁶ Höpfner et al. (2009, 2013). ⁷ HITRAN 2012 spectral line errors: Rothman et al. (2013)

To derive altitude profiles of NH₃ from each averaged limb scan, we have applied a constrained nonlinear multi-parameter least-squares fitting procedure, whereby measurements from all spectra of one limb scan are analyzed in one step (e.g., von Clarmann et al., 2003; Höpfner et al., 2009). The unknown atmospheric state is described in terms of trace gas volume mixing ratios at discrete altitude levels with a grid distance of 1 km. This grid is finer compared to the instrumental vertical field of view width of about 3 km at the tangent points and also finer than the vertical sampling distance of 1.5–3 km. To dampen vertical oscillations arising from the ill-posedness of the inverse problem, a first-order smoothing constraint has been chosen (Tikhonov, 1963; Steck, 2002). The regularization strengths have been adjusted independently for each species being retrieved simultaneously.

For the fitting of the NH₃ signatures we have chosen spectral windows within the interval 950–970 cm⁻¹, which have the advantage that they are situated in the region of one of the optically thinnest mid-infrared atmospheric windows. Furthermore, there are relatively few spectrally interfering species which have to be retrieved simultaneously with NH₃. Spectroscopic line parameters of the HITRAN 2012 database (Rothman et al., 2013) have been used.

A scheme consisting of two steps has been identified as adequate for the retrieval of NH₃. First, the broader wave number range 962–968 cm⁻¹ has been chosen to fit the strong CO₂ lines of the laser band together with the interfering species O₃, H₂O, NH₃, and COF₂. In the second step, narrow analysis windows have been placed around the strongest signatures of NH₃: 951.6–952.0, 965.1–965.6, and 966.6–967.5 cm⁻¹ (MIPAS period 1) and 951.625–952.0, 965.125–965.625, and 966.625–967.5 cm⁻¹ (MIPAS

period 2), thereby avoiding the peaks of the strong CO₂ lines. At this stage CO₂ is kept fixed to the results from the initial retrieval, while O₃, H₂O, and COF₂ are retrieved jointly with NH₃.

Figure 1 presents the spectral fit and the detection of NH₃ for examples from both MIPAS periods at tangent heights around 12.5 km within the region of the Asian monsoon in June–August 2003 (top panel) and 2009 (bottom panel). Within each panel the top row shows the observations in black, the fit without taking NH₃ into account in blue, and the retrieval including NH₃ in red. In the second row of each panel the residual spectra are shown for the retrieval without (blue) and with (red) consideration of NH₃. Here the green line is the difference between the two simulations (with minus without NH₃) in order to show the spectral signature of NH₃ without any instrumental effect, such as spectral noise.

The top panel of Fig. 1 reveals clearly the presence of NH₃ in MIPAS limb spectra. Radiative transfer simulations without a consideration of NH₃ lead to the largest residuals (bold blue curves) at the position of the ammonia lines (dotted orange curves). Only when ammonia is taken into account are the observed spectra within all three microwindows fitted sufficiently well. Comparing the first row of the bottom panel in Fig. 1 with that of the top panel, the worse spectral resolution of MIPAS period 2 becomes obvious. Still the residuals of the NH₃ spectral lines and the better fit upon their consideration are visible, especially in microwindows 2 and 3.

Results of the altitude-dependent error estimation are presented in Fig. 2 for the two examples of the limb scans for which the spectral fits have been shown in Fig. 1. A summary of the assumptions on the various sources of uncertainty is provided in Table 1. For spectral noise, the actual error numbers referring to the two limb scans discussed are

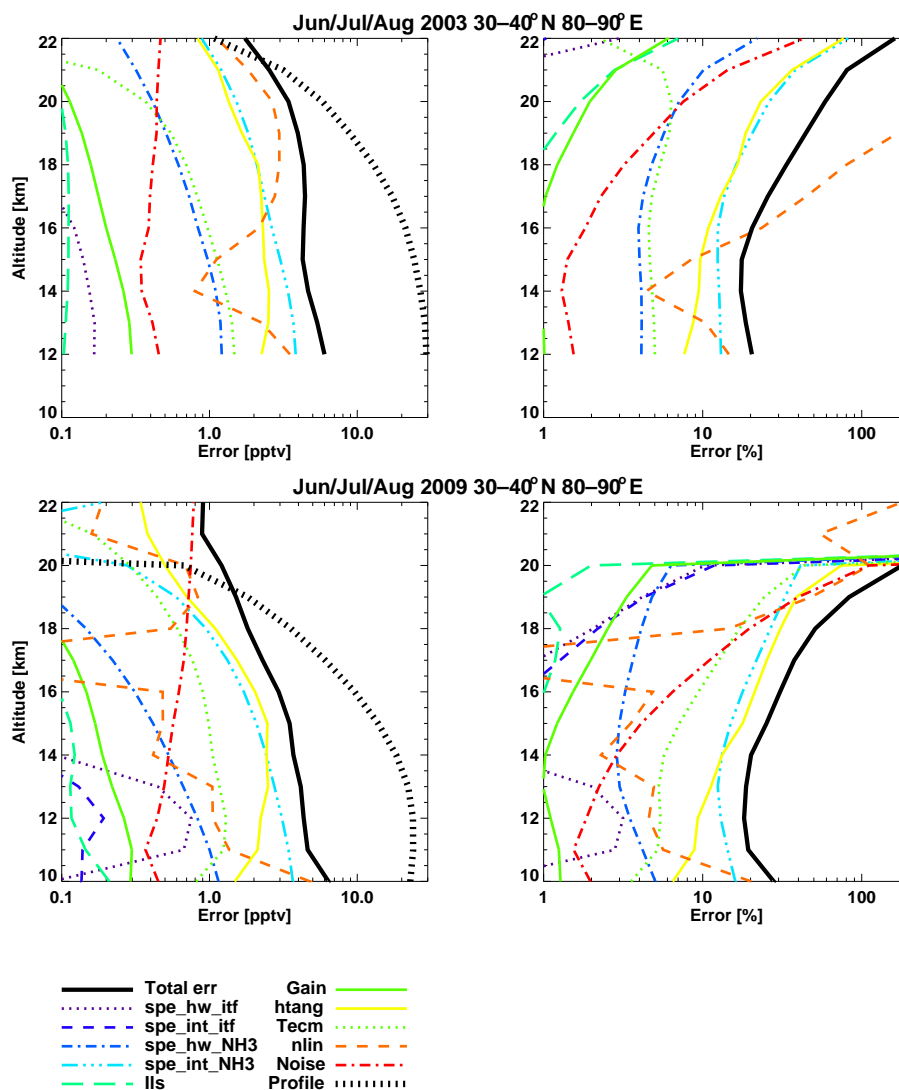


Figure 2. Estimated error profiles for two examples: one from measurement period 1 (June, July, and August 2003; 30–40° N, 80–90° E) and one from period 2 (June, July, and August 2009; 30–40° N, 80–90° E). The retrieved NH₃ profiles are shown as bold black dotted lines (“profile”). Abbreviations of the error sources are resolved in Table 1.

given together with their range over all observations in brackets. While noise is directly mapped into the state space for each individual retrieval, the error estimation for all other uncertainties has been performed by sensitivity calculations for atmospheric conditions representative of observations within the influence of the Asian monsoon (Höpfner et al., 2009, 2013).

In the left panels of Fig. 2 the bold dotted curves indicate the reconstructed vertical profiles of NH₃. The concentrations reach maximum values of around 24–29 pptv. The bold solid lines represent the total error calculated as the square root of the sum of all squared error components. The total errors amount to around 2–6 pptv (17–80 %, right panels) in the altitude region up to about 20 km. Above, the estimated errors are larger than the mixing ratios of NH₃. The leading

error components are tangent altitude uncertainties, uncertainties in the HITRAN line intensity data of NH₃, and non-linearity effects in the averaging procedure as discussed in Höpfner et al. (2009). On the other hand, the use of averaged spectra reduces the noise term to less than 1 pptv within the altitude range of interest.

The vertical resolution of the resulting altitude profiles of NH₃ mixing ratios is directly connected to the noise error values through the applied setting of the regularization strength. The altitude resolution of the retrieval is described by the retrieval averaging kernel matrix (Rodgers, 2000). Examples for both MIPAS periods are provided in Fig. 3. From these, typical vertical resolutions are derived as the retrieval grid width divided by the inverse of the diagonal matrix elements (Rodgers, 2000). The globally average vertical res-

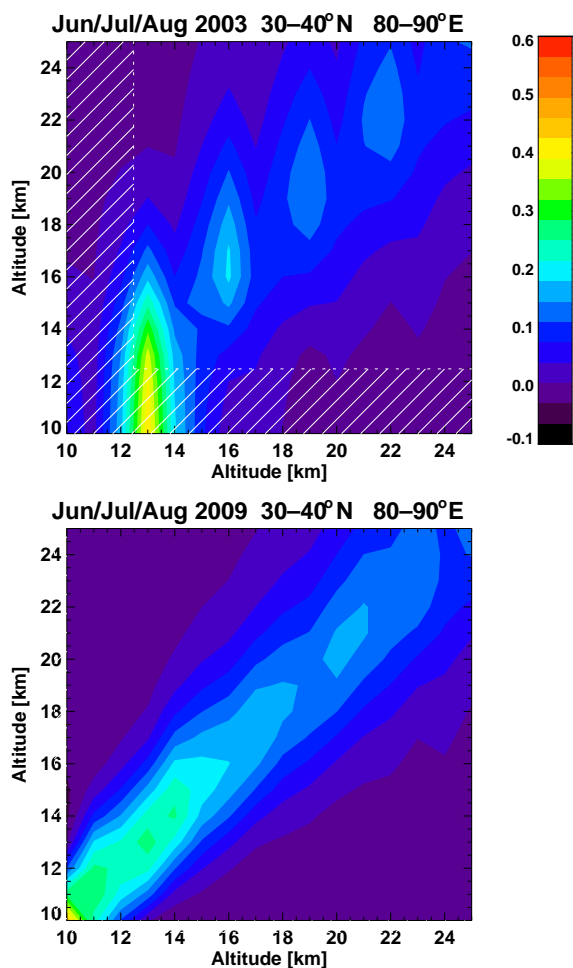


Figure 3. Averaging kernels of the MIPAS NH₃ retrieval during the first (top) and second (bottom) MIPAS measurement period. The number of degrees of freedom up to 25 km is 2.1 (top) and 3.5 (bottom). Hatched areas indicate altitudes below the lowest tangent height where no measurement information is available.

olution at the altitude levels 12, 15, and 18 km, which are discussed in more detail below, is 6.6, 7.9, and 8.8 km during period 1 and 3.5, 4.3, and 5.6 km during period 2.

4 The global dataset

Retrievals of NH₃ have been performed for the entire period of MIPAS observations, i.e., from July 2002 until April 2012. Figure 4 presents the global volume mixing ratio distributions at 15 km altitude during seven seasons from July 2002 until February 2004. There are enhanced values of up to 33 pptv within a region between 30–110° E and 20–50° N during boreal summer, coinciding with the occurrence of the Asian monsoons. During all other seasons of the two MIPAS periods and outside the region influenced by the Asian monsoon, no similarly high concentrations of NH₃ can be

found within the entire altitude region covered by our measurements.

An overview for all years with sufficient data coverage in the Asian summer monsoon season during the MIPAS mission lifetime is provided in Fig. 5 for altitude levels of 12, 15, and 18 km. Due to the less frequent presence of clouds, the number of pixels with valid measurements increases with altitude. Similar to the results from MIPAS period 1, also during period 2 the enhancement of NH₃ within the Asian monsoon region is present for all years of observation. Further, on a global scale there are no other areas visible in the dataset with similarly enhanced values of NH₃. While at 12 and 15 km altitude NH₃ enhancements compared to the global background state are visible during all years, at 18 km altitude increased values of NH₃ are present only during the years 2003, 2008, and 2010.

A comparison between vertical profiles of NH₃ averaged within the western (30–70° E, solid lines) and eastern (70–110° E, dashed lines) parts of the monsoon region for the latitude band 30–40° N is presented in Fig. 6 for the years 2003 and 2007–2011. In the same figure, the dotted curves show the NH₃ mean June, July, and August profiles for all years outside the Asian monsoon area, for the same longitude and latitude range (30–110° E, 30–40° S) of the Southern Hemisphere. The profiles in the region of the Asian monsoon reveal that the maximum concentrations over the whole altitude range within 1 year are always larger in the eastern part of the Asian monsoon compared to the western part. Maximum concentrations of NH₃ in the eastern part reach about 10–22 pptv at 11–13 km altitude. Largest values are found in 2003 and 2009 and lowest ones in 2007 and 2011.

In the western part of the area influenced by the Asian monsoon, enhanced averaged volume mixing ratios of NH₃ can be observed during the years 2003, 2008, and 2010 with values ranging from 6 to 15 pptv. Situated at around 13–15 km, the maximum concentrations in the western part are always located at higher altitudes compared to those from the eastern part of the monsoon region. The position of the NH₃ maximum at higher altitudes in the western compared to the eastern part of the monsoon system might be due to convective uplift of boundary layer air in the east followed by upper-tropospheric transport and further uplift towards the west. Such an uplift of air from east to west is indicated in Vogel et al. (2014, Fig. 10) by trajectory calculations; however, it is mainly located at the border of the anticyclone.

The mean NH₃ profiles of the western part show no clear enhancements during the years 2007, 2009, and 2011. These profiles exhibit maximum values below 5 pptv, which are in the range of concentrations retrieved in the case of the “background” state of the Southern Hemisphere (indicated by dotted lines in Fig. 6). These values are below our estimated detection limit (see below).

Due to the lack of ammonia observations in the upper troposphere, we cannot validate our dataset with correlative measurements. However, in the next section we discuss its

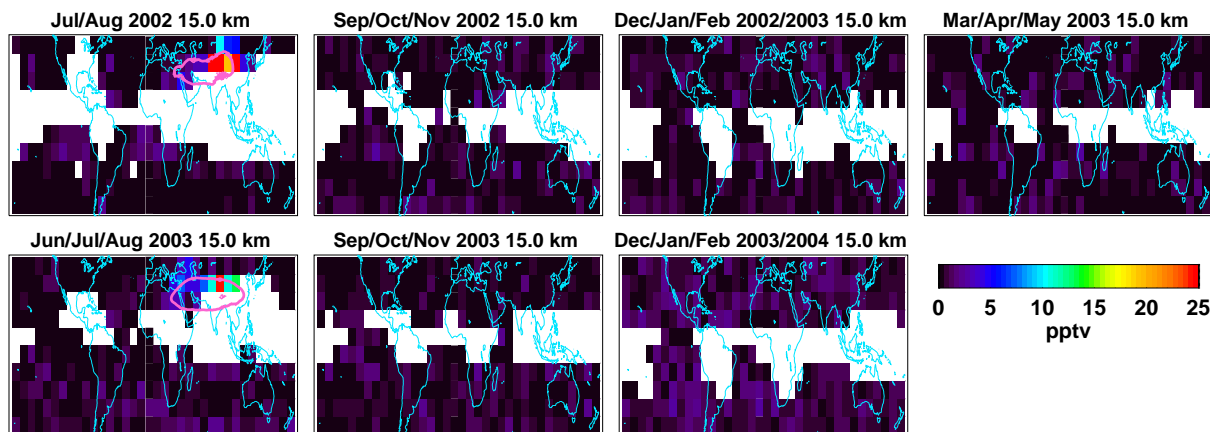


Figure 4. Distributions of NH₃ volume mixing ratios at 15 km altitude between 50° N and 50° S retrieved from MIPAS seasonal mean spectra during the first measurement period. Pixels where not enough spectra for averaging were available are left white. To guide the eye, the pink lines denote the approximate position of the Asian monsoon anticyclone. It is the $2 \times 10^{-6} \text{ K m}^2 \text{ kg}^{-1} \text{ s}^{-1}$ contour of the mean potential vorticity for July and August in 2002 and June, July, and August in 2003 at the potential temperature level of 370 K from the ECMWF ERA interim reanalysis (Dee et al., 2011) (e.g., Ploeger et al., 2015, and references therein).

plausibility by comparing it with the few previous observations and atmospheric model results.

5 Discussion

As mentioned in the introduction, observations of NH₃ reaching upper-tropospheric levels have been published by Ziereis and Arnold (1986). They report upper limits of about 0.04 pptv between 8 and 10 km over Germany in May 1985. At the present state of our MIPAS data analysis, we cannot contradict those upper values outside the influence of the Asian summer monsoon system. Given the total error of a few parts per trillion by volume, we would estimate the 1σ detection limit of our retrieval to be about 3–5 pptv. One might argue that the use of a 1σ detection limit does not provide sufficiently significant evidence of the NH₃ enhancement within the monsoon. However, random errors cannot explain why the enhancements should appear in a contiguous geographical pattern nor could they account for the enhancements appearing only in one season.

For example within the data shown in Fig. 5 at 12 km, there are 176 values larger than 5 pptv outside the region 20–50° N, 30–120° E compared to 55 inside. However, at the 15 km level, only five data points exceed 5 pptv outside but 37 inside. Using 2σ , there are no data points outside compared to 23 and 15 exceeding 10 pptv inside the region at 12 and 15 km, respectively. Further, the detected enhancements inside the monsoon region are in many cases (13 times at 12 km and 8 times at 15 km) even above 15 pptv and, thus, larger than a 3σ limit. Temporally resolved values above 10 pptv in the monsoon region exist during all years at both altitude levels with the exception of 2011 at 15 km. In total, 15 pptv

is exceeded at 10 km in 2003–2010 and at 15 km in all years but 2007 and 2011.

Regarding the retrievals outside the monsoon area, there is a difference between the two MIPAS measurement periods at 10–12 km altitude (see, e.g., the difference in the dotted lines in Fig. 6 or the higher background level at 12 km altitude visible in Fig. 5 between the year 2003 and 2007–2011) that reaches 4 pptv. We attribute this discrepancy to an unexplained systematic uncertainty caused by the different spectral resolutions between the two instrumental states. This observation corroborates our error estimation and supports our conclusion that retrieved values up to 3–5 pptv are below the detection limit of the actual dataset.

Nonetheless, our measurements impose constraints on the global distribution of upper-tropospheric NH₃ concentrations which can be compared to results from model calculations. One of the first globally modeled distributions of NH₃ was presented by Dentener and Crutzen (1994, their Fig. 2b). These calculations were based on the tropospheric transport model Moguntia with a horizontal resolution of $10^\circ \times 10^\circ$ with 10 layers up to 100 hPa in combination with, at that time, the first global emission inventory of NH₃ with the same resolution as the transport model. Yearly mean mixing ratios of below 2 pptv are modeled at upper-tropospheric levels at mid- and high latitudes. These are consistent with the MIPAS background values. However, at equatorial and sub-tropical latitudes, annual mean values of some tens of parts per trillion by volume were simulated between 300 hPa (≈ 9.5 km) and 200 hPa (≈ 12.5 km), which are clearly larger than the MIPAS results. Dentener and Crutzen (1994) attributed these values to natural emissions in the tropics. The comparison with our results indicates that either these emissions might have been overestimated or the tropical sink processes of NH₃ underestimated. In their conclusions Dentener

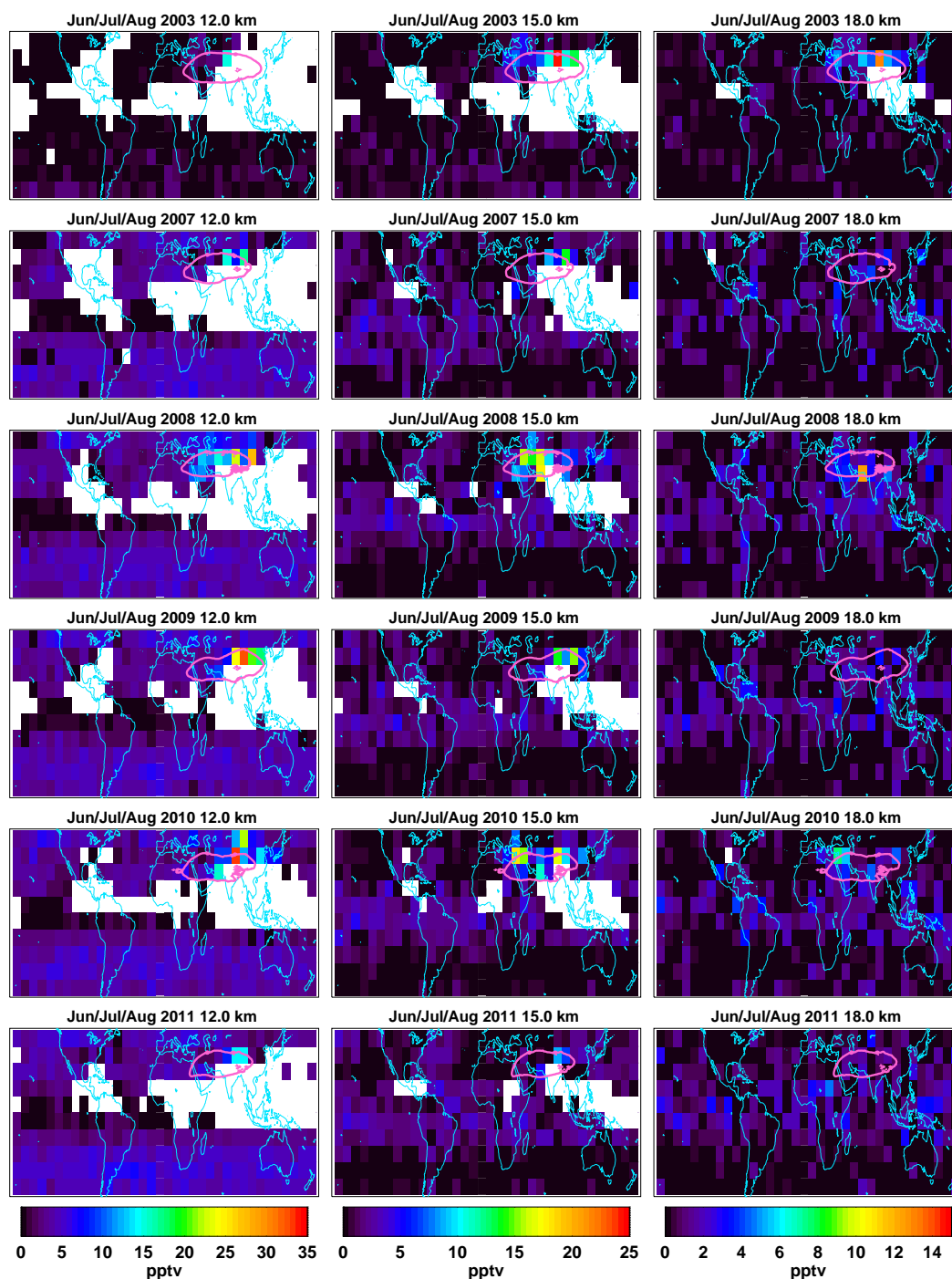


Figure 5. Distributions of NH₃ volume mixing ratios at 12, 15, and 18 km altitude between 50° N and 50° S retrieved from MIPAS seasonal mean spectra during the Asian monsoon period for several years. Pixels where not enough spectra for averaging were available are left white. Pink contour lines denote the mean position of the Asian monsoon anticyclone for June, July, and August as described in the caption of Fig. 4.

and Crutzen (1994) also mention high modeled concentrations of NH₃ in the free troposphere over India and China. However, since these enhancements were not quantified, they cannot be compared to our observations.

In contrast to the results of Dentener and Crutzen (1994), the zonal and yearly averages of modeled NH₃ shown in Feng and Penner (2007, Fig. 9) decrease to well below 10 pptv above 500 hPa (≈ 6 km) also in tropical regions.

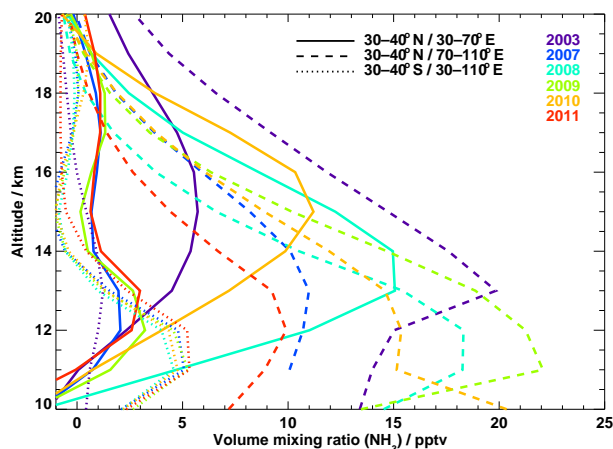


Figure 6. Mean profiles of NH₃ from MIPAS within the geographical range noted in the figure legend during June, July, and August of each year. Solid: western part; dashed: eastern part of the Asian monsoon; dotted: reference profiles outside the monsoon in the Southern Hemisphere.

Their aerosol chemistry transport model (Umich/IMPACT) had a horizontal resolution of 2° latitude × 2.5° longitude with 26 layers up to 0.1 hPa using the 1° × 1° global NH₃ emission inventory of Bouwman et al. (1997). Thus, these global model results are more compatible with the MIPAS dataset.

Globally resolved annual mean model results of NH₃ are given in Adams et al. (1999, Plate 3a). These data were based on runs with the general circulation model GISS GCM II-prime with a 4° latitude × 5° longitude horizontal resolution, nine vertical layers up to 10 hPa and NH₃ emissions according to Bouwman et al. (1997). Mean mixing ratios of about 3.2 pptv at the 200 hPa pressure level ($\approx 12.5/11$ km in tropical/polar regions) are reported. At that pressure level, a slight gradient between the two hemispheres is visible, with values of 0–1 pptv in the south and 3–10 pptv in the north. We do not recognize such a gradient in the background NH₃ concentrations from the MIPAS measurements, although, given our estimated error, we cannot conclusively refute such a gradient.

Regarding ammonium nitrate aerosol during the Asian monsoon season, Metzger et al. (2002) discuss their model results of enhanced values at upper-tropospheric levels over Asia. They used the global chemistry transport model TM3 with 7.5° latitude × 10° longitude horizontal resolution, 19 vertical levels and the EDGAR database for the emissions of NH₃. These high amounts of ammonium nitrate over Asia are attributed to in situ production from NH₃ (and HNO₃) being convectively transported to upper-tropospheric levels. The fact that NH₃ is not removed by dissolution in droplets and subsequent rainout is explained by the low acidity of convective clouds, such that only part of the NH₃ would be dissolved. Our observations support these results with re-

spect to the enhanced amounts of NH₃ which obviously survive the uplift within the Asian monsoon circulation. This indicates that a part of the Asian tropopause aerosol layer (ATAL) (Vernier et al., 2011) might be composed of ammonium nitrate, ammonium sulfate, or other ammonium-containing particles.

Further, through a possible influence of the Asian monsoon on the composition of the tropical tropopause layer (TTL) by transport of ammonia or ammonium, our measurements may help to explain why in situ measurements of aerosols in the TTL indicate that the sulfate appears to be mostly or fully neutralized (Froyd et al., 2009, 2010). Measurements of particle acidity hold potential to inform us about low NH₃ concentrations further in the background UT outside the Asian summer monsoon system.

6 Conclusions

We have presented the first evidence of ammonia being present in the Earth's upper troposphere above 10 km by an analysis of MIPAS infrared limb-emission spectra. The region and period of detection is confined to the Asian summer monsoon system. Maximum average values of around 30 pptv over a 3-month period have been retrieved, thus demonstrating that part of the NH₃ released at the ground survives the loss processes on its way to the upper troposphere. As suggested by Metzger et al. (2002), ammonia may form ammonium nitrate aerosols under those circumstances. Thus, our observations indicate a possible contribution of ammonium aerosols to the composition of the ATAL.

The detection of enhanced amounts of NH₃ in the western part of the Asian monsoon anticyclone during several years suggests that its lifetime is long enough to survive transport to areas far from the source region. The generally lower mixing ratios of NH₃ in the western compared to the eastern part indicate ongoing loss processes at high altitudes.

Unfortunately, in the literature there seem to exist no locally resolved model results of NH₃ during the monsoon period to which we could compare our observations. We anticipate that such simulations would be of value to improve our understanding of NH₃ loss processes and aerosol production in the Asian monsoon. Also, airborne remote-sensing observations, like the one planned within the EU project StratoClim with the GLORIA instrument on the Geophysica high flying aircraft, would strongly increase our knowledge about ammonia distributions in the Asian monsoon on a much finer time, horizontal, and vertical resolution scale than the MIPAS dataset presented here.

Regarding the global distribution of upper-tropospheric NH₃ outside the Asian monsoon, within this study we could provide upper limits in the range of a few parts per trillion by volume. This will help to constrain global models and to improve their results.

7 Data availability

The NH₃ dataset is available upon request from the author or at <http://www.imk-asf.kit.edu/english/308.php>.

The Supplement related to this article is available online at doi:10.5194/acp-16-14357-2016-supplement.

Acknowledgements. We thank Michelle Santee, a second reviewer, and the editor Rolf Müller for their constructive comments and Bärbel Vogel for helpful discussions. Provision of MIPAS level-1b calibrated spectra by ESA and meteorological analysis data by ECMWF is acknowledged. The research leading to these results has received funding from the European Community's Seventh Framework Programme (FP7/2007–2013) under grant agreement 603557. Rainer Volkamer is recipient of a KIT Distinguished Intl Scholar award, and acknowledges funding from the US National Science Foundation EAGER award AGS-1452317. We acknowledge support by the Deutsche Forschungsgemeinschaft and the Open Access Publishing Fund of the Karlsruhe Institute of Technology.

The article processing charges for this open-access publication were covered by a Research Centre of the Helmholtz Association.

Edited by: R. Müller

Reviewed by: M. Santee and one anonymous referee

References

- Abbatt, J. P. D., Benz, S., Cziczo, D. J., Kanji, Z., Lohmann, U., and Möhler, O.: Solid Ammonium Sulfate Aerosols as Ice Nuclei: A Pathway for Cirrus Cloud Formation, *Science*, doi:10.1126/science.1129726, 2006.
- Adams, P. J., Seinfeld, J. H., and Koch, D. M.: Global concentrations of tropospheric sulfate, nitrate, and ammonium aerosol simulated in a general circulation model, *J. Geophys. Res.*, 104, 13791–13823, 1999.
- Adams, P. J., Seinfeld, J. H., Koch, D., Mickley, L., and Jacob, D.: General circulation model assessment of direct radiative forcing by the sulfate-nitrate-ammonium-water inorganic aerosol system, *J. Geophys. Res.*, 106, 1097–1111, 2001.
- Beer, R., Shephard, M. W., Kulawik, S. S., Clough, S. A., Eldering, A., Bowman, K. W., Sander, S. P., Fisher, B. M., Payne, V. H., Luo, M., Osterman, G. B., and Worden, J. R.: First satellite observations of lower tropospheric ammonia and methanol, *Geophys. Res. Lett.*, 35, L09801, doi:10.1029/2008GL033642, 2008.
- Behera, S. N., Sharma, M., Aneja, V. P., and Balasubramanian, R.: Ammonia in the atmosphere: a review on emission sources, atmospheric chemistry and deposition on terrestrial bodies, *Environ. Sci. Pollut. Res.*, 20, 8092–8131, 2013.
- Bellouin, N., Rae, J., Jones, A., Johnson, C., Haywood, J., and Boucher, O.: Aerosol forcing in the Climate Model Intercomparison Project (CMIP5) simulations by HadGEM2-ES and the role of ammonium nitrate, *J. Geophys. Res.*, 116, D20206, doi:10.1029/2011JD016074, 2011.
- Boucher, O., Randall, D., Artaxo, P., Bretherton, C., Feingold, G., Forster, P., Kerminen, V.-M., Kondo, Y., Liao, H., Lohmann, U., Rasch, P., Satheesh, S., Sherwood, S., Stevens, B., and Zhang, X.: *Clouds and Aerosols*, Cambridge University Press, Cambridge, United Kingdom and New York, NY, USA, 2013.
- Bouwman, A., Lee, D., Asman, W., Dentener, F., Van Der Hoek, K., and Olivier, J.: A global high-resolution emission inventory for ammonia, *Global Biogeochem. Cy.*, 11, 561–587, 1997.
- Burgess, A., Dudhia, A., Grainger, R., and Stevenson, D.: Progress in tropospheric ammonia retrieval from the {MIPAS} satellite instrument, *Adv. Space Res.*, 37, 2218–2221, 2006.
- Clarisse, L., Clerbaux, C., Dentener, F., Hurtmans, D., and Coheur, P.-F.: Global ammonia distribution derived from infrared satellite observations, *Nat. Geosci.*, 2, 479–483, 2009.
- Clarisse, L., Shephard, M. W., Dentener, F., Hurtmans, D., Cady-Pereira, K., Karagulian, F., Van Damme, M., Clerbaux, C., and Coheur, P.-F.: Satellite monitoring of ammonia: A case study of the San Joaquin Valley, *J. Geophys. Res.*, 115, D13302, doi:10.1029/2009JD013291, 2010.
- Coheur, P.-F., Herbin, H., Clerbaux, C., Hurtmans, D., Wespes, C., Carleer, M., Turquety, S., Rinsland, C. P., Remedios, J., Hauglustaine, D., Boone, C. D., and Bernath, P. F.: ACE-FTS observation of a young biomass burning plume: first reported measurements of C₂H₄, C₃H₆O, H₂CO and PAN by infrared occultation from space, *Atmos. Chem. Phys.*, 7, 5437–5446, doi:10.5194/acp-7-5437-2007, 2007.
- Coheur, P.-F., Clarisse, L., Turquety, S., Hurtmans, D., and Clerbaux, C.: IASI measurements of reactive trace species in biomass burning plumes, *Atmos. Chem. Phys.*, 9, 5655–5667, doi:10.5194/acp-9-5655-2009, 2009.
- Dammers, E., Vigouroux, C., Palm, M., Mahieu, E., Warneke, T., Smale, D., Langerock, B., Franco, B., Van Damme, M., Schaap, M., Notholt, J., and Erisman, J. W.: Retrieval of ammonia from ground-based FTIR solar spectra, *Atmos. Chem. Phys.*, 15, 12789–12803, doi:10.5194/acp-15-12789-2015, 2015.
- Dammers, E., Palm, M., Van Damme, M., Vigouroux, C., Smale, D., Conway, S., Toon, G. C., Jones, N., Nussbaumer, E., Warneke, T., Petri, C., Clarisse, L., Clerbaux, C., Hermans, C., Lutsch, E., Strong, K., Hannigan, J. W., Nakajima, H., Morino, I., Herrera, B., Stremme, W., Grutter, M., Schaap, M., Wichink Kruit, R. J., Notholt, J., Coheur, P.-F., and Erisman, J. W.: An evaluation of IASI-NH₃ with ground-based Fourier transform infrared spectroscopy measurements, *Atmos. Chem. Phys.*, 16, 10351–10368, doi:10.5194/acp-16-10351-2016, 2016.
- Dee, D. P., Uppala, S. M., Simmons, A. J., Berrisford, P., Poli, P., Kobayashi, S., Andrae, U., Balmaseda, M. A., Balsamo, G., Bauer, P., Bechtold, P., Beljaars, A. C. M., van de Berg, L., Bidlot, J., Bormann, N., Delsol, C., Dragani, R., Fuentes, M., Geer, A. J., Haimberger, L., Healy, S. B., Hersbach, H., Hólm, E. V., Isaksen, I., Kållberg, P., Köhler, M., Matricardi, M., McNally, A. P., Monge-Sanz, B. M., Morcrette, J.-J., Park, B.-K., Peubey, C., de Rosnay, P., Tavolato, C., Thépaut, J.-N., and Vitart, F.: The ERA-Interim reanalysis: configuration and performance of the data assimilation system, *QJRMS*, 137, 553–597, 2011.
- Dentener, F. J. and Crutzen, P. J.: A three-dimensional model of the global ammonia cycle, *J. Atmos. Chem.*, 19, 331–369, 1994.

- Erisman, J. W., Sutton, M. A., Galloway, J., Klimont, Z., and Winiwarter, W.: How a century of ammonia synthesis changed the world, *Nat. Geosci.*, 1, 636–639, doi:10.1038/ngeo325, 2008.
- Feng, Y. and Penner, J. E.: Global modeling of nitrate and ammonium: Interaction of aerosols and tropospheric chemistry, *J. Geophys. Res.*, 112, D01304, doi:10.1029/2005JD006404, 2007.
- Fischer, H., Birk, M., Blom, C., Carli, B., Carlotti, M., von Clarmann, T., Delbouille, L., Dudhia, A., Ehhalt, D., Endemann, M., Flaud, J. M., Gessner, R., Kleinert, A., Koopman, R., Langen, J., López-Puertas, M., Mosner, P., Nett, H., Oelhaf, H., Perron, G., Remedios, J., Ridolfi, M., Stiller, G., and Zander, R.: MIPAS: an instrument for atmospheric and climate research, *Atmos. Chem. Phys.*, 8, 2151–2188, doi:10.5194/acp-8-2151-2008, 2008.
- Forster, P., Ramaswamy, V., Artaxo, P., Bernsten, T., Betts, R., Fahey, D., Haywood, J., Lean, J., Lowe, D., Myhre, G., Nganga, J., Prinn, R., Raga, G., Schulz, M., and Van Dorland, R.: Changes in Atmospheric Constituents and in Radiative Forcing, Cambridge University Press, Cambridge, United Kingdom and New York, NY, USA, 129–243, 2007.
- Froyd, K. D., Murphy, D. M., Sanford, T. J., Thomson, D. S., Wilson, J. C., Pfister, L., and Lait, L.: Aerosol composition of the tropical upper troposphere, *Atmos. Chem. Phys.*, 9, 4363–4385, doi:10.5194/acp-9-4363-2009, 2009.
- Froyd, K. D., Murphy, D. M., Lawson, P., Baumgardner, D., and Herman, R. L.: Aerosols that form subvisible cirrus at the tropical tropopause, *Atmos. Chem. Phys.*, 10, 209–218, doi:10.5194/acp-10-209-2010, 2010.
- Hamaoui-Laguel, L., Meleux, F., Beekmann, M., Bessagnet, B., Générmont, S., Cellier, P., and Létinois, L.: Improving ammonia emissions in air quality modelling for France, *Atmos. Environ.*, 92, 584–595, 2014.
- Hauglustaine, D. A., Balkanski, Y., and Schulz, M.: A global model simulation of present and future nitrate aerosols and their direct radiative forcing of climate, *Atmos. Chem. Phys.*, 14, 11031–11063, doi:10.5194/acp-14-11031-2014, 2014.
- Höpfner, M., von Clarmann, T., Fischer, H., Funke, B., Glatthor, N., Grabowski, U., Kellmann, S., Kiefer, M., Linden, A., Milz, M., Steck, T., Stiller, G. P., Bernath, P., Blom, C. E., Blumenstock, Th., Boone, C., Chance, K., Coffey, M. T., Friedl-Vallon, F., Griffith, D., Hannigan, J. W., Hase, F., Jones, N., Jucks, K. W., Keim, C., Kleinert, A., Kouker, W., Liu, G. Y., Mahieu, E., Mellqvist, J., Mikuteit, S., Notholt, J., Oelhaf, H., Piesch, C., Reddman, T., Ruhnke, R., Schneider, M., Strandberg, A., Toon, G., Walker, K. A., Warneke, T., Wetzell, G., Wood, S., and Zander, R.: Validation of MIPAS ClONO₂ measurements, *Atmos. Chem. Phys.*, 7, 257–281, doi:10.5194/acp-7-257-2007, 2007.
- Höpfner, M., Orphal, J., von Clarmann, T., Stiller, G., and Fischer, H.: Stratospheric BrONO₂ observed by MIPAS, *Atmos. Chem. Phys.*, 9, 1735–1746, doi:10.5194/acp-9-1735-2009, 2009.
- Höpfner, M., Glatthor, N., Grabowski, U., Kellmann, S., Kiefer, M., Linden, A., Orphal, J., Stiller, G., von Clarmann, T., Funke, B., and Boone, C. D.: Sulfur dioxide (SO₂) as observed by MIPAS/Envisat: temporal development and spatial distribution at 15–45 km altitude, *Atmos. Chem. Phys.*, 13, 10405–10423, doi:10.5194/acp-13-10405-2013, 2013.
- Kiefer, M., von Clarmann, T., Grabowski, U., De Laurentis, M., Mantovani, R., Milz, M., and Ridolfi, M.: Characterization of MIPAS elevation pointing, *Atmos. Chem. Phys.*, 7, 1615–1628, doi:10.5194/acp-7-1615-2007, 2007.
- Kirkby, J., Curtius, J., Almeida, J., Dunne, E., Duplissy, J., Ehrhart, S., Franchin, A., Gagné, S., Ickes, L., Kürten, A., Kupc, A., Metzger, A., Riccobono, F., Rondo, L., Schobesberger, S., Tsagkogeorgas, G., Wimmer, D., Amorim, A., Bianchi, F., Breitenlechner, M., David, A., Dommen, J., Downard, A., Ehn, M., Flagan, R. C., Haider, S., Hansel, A., Hauser, D., Jud, W., Junninen, H., Kreissl, F., Kvashin, A., Laaksonen, A., Lehtipalo, K., Lima, J., Lovejoy, E. R., Makhmutov, V., Mathot, S., Mikkilä, J., Minginette, P., Mogo, S., Nieminen, T., Onnela, A., Pereira, P., Petäjä, T., Schnitzhofer, R., Seinfeld, J. H., Sipilä, M., Stozhkov, Y., Stratmann, F., Tomé, A., Vanhanen, J., Viisanen, Y., Vrtala, A., Wagner, P. E., Walther, H., Weingartner, E., Wex, H., Winkler, P. M., Carslaw, K. S., Worsnop, D. R., Baltensperger, U., and Kulmala, M.: Role of sulphuric acid, ammonia and galactic cosmic rays in atmospheric aerosol nucleation, *Nature*, 476, 429–433, 2011.
- Kleinert, A., Aubertin, G., Perron, G., Birk, M., Wagner, G., Hase, F., Nett, H., and Poulin, R.: MIPAS Level 1B algorithms overview: operational processing and characterization, *Atmos. Chem. Phys.*, 7, 1395–1406, doi:10.5194/acp-7-1395-2007, 2007.
- Kürten, A., Münch, S., Rondo, L., Bianchi, F., Duplissy, J., Jokinen, T., Junninen, H., Sarnela, N., Schobesberger, S., Simon, M., Sipilä, M., Almeida, J., Amorim, A., Dommen, J., Donahue, N. M., Dunne, E. M., Flagan, R. C., Franchin, A., Kirkby, J., Kupc, A., Makhmutov, V., Petäjä, T., Praplan, A. P., Riccobono, F., Steiner, G., Tomé, A., Tsagkogeorgas, G., Wagner, P. E., Wimmer, D., Baltensperger, U., Kulmala, M., Worsnop, D. R., and Curtius, J.: Thermodynamics of the formation of sulfuric acid dimers in the binary (H₂SO₄-H₂O) and ternary (H₂SO₄-H₂O-NH₃) system, *Atmos. Chem. Phys.*, 15, 10701–10721, doi:10.5194/acp-15-10701-2015, 2015.
- Leen, J. B., Yu, X.-Y., Gupta, M., Baer, D. S., Hubbe, J. M., Kluzek, C. D., Tomlinson, J. M., and Mike R. Hubbell, I.: Fast In Situ Airborne Measurement of Ammonia Using a Mid-Infrared Off-Axis ICOS Spectrometer, *Environ. Sci. Technol.*, 47, 10446–10453, doi:10.1021/es401134u, 2013.
- Liao, H. and Seinfeld, J. H.: Global impacts of gas-phase chemistry-aerosol interactions on direct radiative forcing by anthropogenic aerosols and ozone, *J. Geophys. Res.*, 110, D18208, doi:10.1029/2005JD005907, 2005.
- Martin, S. T., Hung, H.-M., Park, R. J., Jacob, D. J., Spurr, R. J. D., Chance, K. V., and Chin, M.: Effects of the physical state of tropospheric ammonium-sulfate-nitrate particles on global aerosol direct radiative forcing, *Atmos. Chem. Phys.*, 4, 183–214, doi:10.5194/acp-4-183-2004, 2004.
- Metzger, S., Dentener, F., Krol, M., Jeuken, A., and Lelieveld, J.: Gas/aerosol partitioning 2. Global modeling results, *J. Geophys. Res.*, 107, 1–23, doi:10.1029/2001JD001103, 2002.
- Nowak, J. B., Neuman, J. A., Kozai, K., Huey, L. G., Tanner, D. J., Holloway, J. S., Ryerson, T. B., Frost, G. J., McKeen, S. A., and Fehsenfeld, F. C.: A chemical ionization mass spectrometry technique for airborne measurements of ammonia, *J. Geophys. Res.*, 112, D10S02, doi:10.1029/2006JD007589, 2007.
- Nowak, J. B., Neuman, J. A., Bahreini, R., Brock, C. A., Middlebrook, A. M., Wollny, A. G., Holloway, J. S., Peischl, J., Ryerson, T. B., and Fehsenfeld, F. C.: Airborne observations of ammonia and ammonium nitrate formation over Houston, Texas, *J. Geophys. Res.*, 115, D22304, doi:10.1029/2010JD014195, 2010.

- Nowak, J. B., Neuman, J. A., Bahreini, R., Middlebrook, A. M., Holloway, J. S., McKeen, S. A., Parrish, D. D., Ryerson, T. B., and Trainer, M.: Ammonia sources in the California South Coast Air Basin and their impact on ammonium nitrate formation, *Geophys. Res. Lett.*, 39, 107804, doi:10.1029/2012GL051197, 2012.
- Oelhaf, H., Leupolt, A., and Fischer, H.: Discrepancies between balloon-borne IR atmospheric spectra and corresponding synthetic spectra calculated line by line around 825 cm⁻¹, *Appl. Opt.*, 22, 647–649, 1983.
- Ortega, I. K., Kurtén, T., Vehkamäki, H., and Kulmala, M.: The role of ammonia in sulfuric acid ion induced nucleation, *Atmos. Chem. Phys.*, 8, 2859–2867, doi:10.5194/acp-8-2859-2008, 2008.
- Paulot, F., Jacob, D. J., Pinder, R. W., Bash, J. O., Travis, K., and Henze, D. K.: Ammonia emissions in the United States, European Union, and China derived by high-resolution inversion of ammonium wet deposition data: Interpretation with a new agricultural emissions inventory (MASAGE_NH3), *J. Geophys. Res.*, 119, 4343–4364, 2014.
- Paulot, F., Jacob, D. J., Johnson, M. T., Bell, T. G., Baker, A. R., Keene, W. C., Lima, I. D., Doney, S. C., and Stock, C. A.: Global oceanic emission of ammonia: Constraints from seawater and atmospheric observations, *Global Biogeochem. Cy.*, 29, 1165–1178, 2015.
- Paulot, F., Ginoux, P., Cooke, W. F., Donner, L. J., Fan, S., Lin, M.-Y., Mao, J., Naik, V., and Horowitz, L. W.: Sensitivity of nitrate aerosols to ammonia emissions and to nitrate chemistry: implications for present and future nitrate optical depth, *Atmos. Chem. Phys.*, 16, 1459–1477, doi:10.5194/acp-16-1459-2016, 2016.
- Ploeger, F., Gottschling, C., Griessbach, S., Groß, J.-U., Guenther, G., Konopka, P., Müller, R., Riese, M., Stroh, F., Tao, M., Ungermann, J., Vogel, B., and von Hobe, M.: A potential vorticity-based determination of the transport barrier in the Asian summer monsoon anticyclone, *Atmos. Chem. Phys.*, 15, 13145–13159, doi:10.5194/acp-15-13145-2015, 2015.
- Prenni, A. J., Wise, M. E., Brooks, S. D., and Tolbert, M. A.: Ice nucleation in sulfuric acid and ammonium sulfate particles, *J. Geophys. Res.-Atmos.*, 106, 3037–3044, 2001.
- Rodgers, C. D.: *Inverse Methods for Atmospheric Sounding: Theory and Practice*, Series on Atmospheric, Oceanic and Planetary Physics, World Scientific, 2, 2000.
- Rothman, L., Gordon, I., Babikov, Y., Barbe, A., Benner, D. C., Bernath, P., Birk, M., Bizzocchi, L., Boudon, V., Brown, L., Campargue, A., Chance, K., Cohen, E., Coudert, L., Devi, V., Drouin, B., Fayt, A., Flaud, J.-M., Gamache, R., Harrison, J., Hartmann, J.-M., Hill, C., Hodges, J., Jacquemart, D., Jolly, A., Lamouroux, J., Roy, R. L., Li, G., Long, D., Lyulin, O., Mackie, C., Massie, S., Mikhailenko, S., Müller, H., Naumenko, O., Nikitin, A., Orphal, J., Perevalov, V., Perrin, A., Polovtseva, E., Richard, C., Smith, M., Starikova, E., Sung, K., Tashkun, S., Tennyson, J., Toon, G., Tyuterev, V., and Wagner, G.: The {HITRAN2012} molecular spectroscopic database, *J. Quant. Spectrosc. Radiat. Transfer*, 130, 4–50, doi:10.1016/j.jqsrt.2013.07.002, 2013.
- Schiferl, L. D., Heald, C. L., Van Damme, M., Clarisse, L., Clerbaux, C., Coheur, P.-F., Nowak, J. B., Neuman, J. A., Herton, S. C., Roscioli, J. R., and Eilerman, S. J.: Interannual variability of ammonia concentrations over the United States: sources and implications, *Atmos. Chem. Phys.*, 16, 12305–12328, doi:10.5194/acp-16-12305-2016, 2016.
- Schobesberger, S., Junninen, H., Bianchi, F., Lönn, G., Ehn, M., Lehtipalo, K., Dommen, J., Ehrhart, S., Ortega, I. K., Franchin, A., Nieminen, T., Riccobono, F., Hutterli, M., Duplissy, J., Almeida, J., Amorim, A., Breitenlechner, M., Downard, A. J., Dunne, E. M., Flagan, R. C., Kajos, M., Keskinen, H., Kirkby, J., Kupc, A., Kürten, A., Kurtén, T., Laaksonen, A., Mathot, S., Onnela, A., Praplan, A. P., Rondo, L., Santos, F. D., Schallhart, S., Schnitzhofer, R., Sipilä, M., Tomé, A., Tsagkogeorgas, G., Vehkamäki, H., Wimmer, D., Baltensperger, U., Carslaw, K. S., Curtius, J., Hansel, A., Petäjä, T., Kulmala, M., Donahue, N. M., and Worsnop, D. R.: Molecular understanding of atmospheric particle formation from sulfuric acid and large oxidized organic molecules, *PNAS*, 110, 17223–17228, 2013.
- Shephard, M. W. and Cady-Pereira, K. E.: Cross-track Infrared Sounder (CrIS) satellite observations of tropospheric ammonia, *Atmos. Meas. Techn.*, 8, 1323–1336, doi:10.5194/amt-8-1323-2015, 2015.
- Shephard, M. W., Cady-Pereira, K. E., Luo, M., Henze, D. K., Pinder, R. W., Walker, J. T., Rinsland, C. P., Bash, J. O., Zhu, L., Payne, V. H., and Clarisse, L.: TES ammonia retrieval strategy and global observations of the spatial and seasonal variability of ammonia, *Atmos. Chem. Phys.*, 11, 10743–10763, doi:10.5194/acp-11-10743-2011, 2011.
- Shindell, D. T., Lamarque, J.-F., Schulz, M., Flanner, M., Jiao, C., Chin, M., Young, P. J., Lee, Y. H., Rotstayn, L., Mahowald, N., Milly, G., Faluvegi, G., Balkanski, Y., Collins, W. J., Conley, A. J., Dalsoren, S., Easter, R., Ghan, S., Horowitz, L., Liu, X., Myhre, G., Nagashima, T., Naik, V., Rumbold, S. T., Skeie, R., Sudo, K., Szopa, S., Takemura, T., Voulgarakis, A., Yoon, J.-H., and Lo, F.: Radiative forcing in the ACCMIP historical and future climate simulations, *Atmos. Chem. Phys.*, 13, 2939–2974, doi:10.5194/acp-13-2939-2013, 2013.
- Spang, R., Remedios, J. J., and Barkley, M. P.: Colour indices for the detection and differentiation of cloud types in infra-red limb emission spectra, *Adv. Space Res.*, 33, 1041–1047, 2004.
- Steck, T.: Methods for determining regularization for atmospheric retrieval problems, *Appl. Opt.*, 41, 1788–1797, 2002.
- Sutton, M. A., Reis, S., Riddick, S. N., Dragosits, U., Nemitz, E., Theobald, M. R., Tang, Y. S., Braban, C. F., Viena, M., Dore, A. J., Mitchell, R. F., Wanless, S., Daunt, F., Fowler, D., Blackall, T. D., Milford, C., Flechard, C. R., Loubet, B., Massad, R., Cellier, P., Personne, E., Coheur, P. F., Clarisse, L., Van Damme, M., Ngadi, Y., Clerbaux, C., Skjøth, C. A., Geels, C., Hertel, O., Wichink Kruit, R. J., Pinder, R. W., Bash, J. O., Walker, J. T., Simpson, D., Horváth, L., Misselbrook, T. H., Bleeker, A., Dentener, F., and de Vries, W.: Towards a climate-dependent paradigm of ammonia emission and deposition, *Philos. T. R. Soc. Lond. B*, 368, 20130166, doi:10.1098/rstb.2013.0166, 2013.
- Tabazadeh, A. and Toon, O. B.: The role of ammoniated aerosols in cirrus cloud nucleation, *Geophys. Res. Lett.*, 25, 1379–1382, 1998.
- Tikhonov, A.: On the solution of incorrectly stated problems and method of regularization, *Dokl. Akad. Nauk. SSSR*, 151, 501–504, 1963.
- Van Damme, M., Clarisse, L., Heald, C. L., Hurtmans, D., Ngadi, Y., Clerbaux, C., Dolman, A. J., Erisman, J. W., and Coheur, P. F.: Global distributions, time series and error characterization

- of atmospheric ammonia (NH₃) from IASI satellite observations, *Atmos. Chem. Phys.*, 14, 2905–2922, doi:10.5194/acp-14-2905-2014, 2014.
- Van Damme, M., Erismann, J. W., Clarisse, L., Dammers, E., Whitburn, S., Clerbaux, C., Dolman, A. J., and Coheur, P.-F.: World-wide spatiotemporal atmospheric ammonia (NH₃) columns variability revealed by satellite, *Geophys. Res. Lett.*, 42, 8660–8668, 2015.
- Vernier, J.-P., Thomason, L. W., and Kar, J.: CALIPSO detection of an Asian tropopause aerosol layer, *Geophys. Res. Lett.*, 38, L07804, doi:10.1029/2010GL046614, 2011.
- Vogel, B., Günther, G., Müller, R., Grooß, J.-U., Hoor, P., Krämer, M., Müller, S., Zahn, A., and Riese, M.: Fast transport from Southeast Asia boundary layer sources to northern Europe: rapid uplift in typhoons and eastward eddy shedding of the Asian monsoon anticyclone, *Atmos. Chem. Phys.*, 14, 12745–12762, doi:10.5194/acp-14-12745-2014, 2014.
- von Bobruzki, K., Braban, C. F., Famulari, D., Jones, S. K., Blackall, T., Smith, T. E. L., Blom, M., Coe, H., Gallagher, M., Ghaliyeni, M., McGillen, M. R., Percival, C. J., Whitehead, J. D., Ellis, R., Murphy, J., Mohacsi, A., Pogany, A., Junninen, H., Rantanen, S., Sutton, M. A., and Nemitz, E.: Field inter-comparison of eleven atmospheric ammonia measurement techniques, *Atmos. Meas. Techn.*, 3, 91–112, doi:10.5194/amt-3-91-2010, 2010.
- von Clarmann, T., Glatthor, N., Grabowski, U., Höpfner, M., Kellmann, S., Kiefer, M., Linden, A., Mengistu Tsidu, G., Milz, M., Steck, T., Stiller, G. P., Wang, D. Y., Fischer, H., Funke, B., Gil-López, S., and López-Puertas, M.: Retrieval of temperature and tangent altitude pointing from limb emission spectra recorded from space by the Michelson Interferometer for Passive Atmospheric Sounding (MIPAS), *J. Geophys. Res.*, 108, 4736, doi:10.1029/2003JD003602, 2003.
- Von Clarmann, T., Höpfner, M., Kellmann, S., Linden, A., Chauhan, S., Funke, B., Grabowski, U., Glatthor, N., Kiefer, M., Schieferdecker, T., Stiller, G. P., and Versick, S.: Retrieval of temperature, H₂O, O₃, HNO₃, CH₄, N₂O, ClONO₂ and ClO from MIPAS reduced resolution nominal mode limb emission measurements, *Atmos. Meas. Tech.*, 2, 159–175, doi:10.5194/amt-2-159-2009, 2009.
- Vuuren, D. P., Edmonds, J., Kainuma, M., Riahi, K., Thomson, A., Hibbard, K., Hurtt, G. C., Kram, T., Krey, V., Lamarque, J.-F., Masui, T., Meinshausen, M., Nakicenovic, N., Smith, S. J., and Rose, S. K.: The representative concentration pathways: an overview, *Climatic Change*, 109, 5–31, 2011.
- Wang, J., Hoffmann, A. A., Park, R. J., Jacob, D. J., and Martin, S. T.: Global distribution of solid and aqueous sulfate aerosols: Effect of the hysteresis of particle phase transitions, *J. Geophys. Res.*, 113, D11206, doi:10.1029/2007JD009367, 2008.
- Warner, J. X., Wei, Z., Strow, L. L., Dickerson, R. R., and Nowak, J. B.: The global tropospheric ammonia distribution as seen in the 13-year AIRS measurement record, *Atmos. Chem. Phys.*, 16, 5467–5479, doi:10.5194/acp-16-5467-2016, 2016.
- Wise, M. E., Garland, R. M., and Tolbert, M. A.: Ice nucleation in internally mixed ammonium sulfate/dicarboxylic acid particles, *J. Geophys. Res.-Atmos.*, 109, D19203, doi:10.1029/2003JD004313, 2004.
- Xu, L. and Penner, J. E.: Global simulations of nitrate and ammonium aerosols and their radiative effects, *Atmos. Chem. Phys.*, 12, 9479–9504, doi:10.5194/acp-12-9479-2012, 2012.
- Ziereis, H. and Arnold, F.: Gaseous ammonia and ammonium ions in the free troposphere, *Nature*, 321, 503–505, 1986.